ACS OMEGA

http://pubs.acs.org/journal/acsodf

Article

Fabrication of Porous Fe-Based Metal–Organic Complex for the Enhanced Delivery of 5-Fluorouracil in In Vitro Treatment of Cancer Cells

Bac Thanh Le, Chau Que Nguyen, Phuong Thi Nguyen, Ha Duc Ninh, Tri Minh Le, Phuong Thi Hoai Nguyen,* and Duong Duc La*

Cite This: *ACS Omega* 2022, 7, 46674–46681

Read Online

ACCESS | Metrics & More | Article Recommendations | Supporting Information

ABSTRACT: Metal–organic complexes are one of the most studied materials in the last few decades, which are fabricated from organic ligands and metal ions to form robust frameworks with porous structures. In this work, iron-1,4-benzenedicarboxylic-polyethylene glycol (Fe-BDC-PEG) with a porous structure was successfully constructed by an iron(III) benzene dicarboxylate and polyethylene glycol diacid. The drug-delivery properties of the resultant Fe-BDC-PEG were tested for the loading and release of the 5-fluorouracil compound. The maximal loading capacity of Fe-BDC-PEG for 5-fluorouracil was determined to be 348.22 mg/g. The drug release of 5-fluorouracil-loaded Fe-BDC-PEG after 7 days was 92.69% and reached a maximum of 97.52% after 10 days. The 7 day and acute oral toxicity of Fe-BDC-PEG in mice were studied. The results show that no reasonable change or mortality was observed upon administration of Fe-BDC-PEG complex in mice at 10 g/kg body weight. When the uptake of Fe-BDC-PEG particles in mice was continued for 7 consecutive days, the mortality, feed consumption, body weight, and daily activity were negligibly changed.

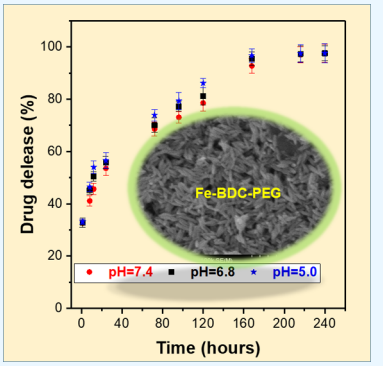

INTRODUCTION

According to the WHO report in 2012, the burden of cancer deaths is second only after cardiovascular disease. Cancer is the cause of 18% of deaths in Vietnam. According to statistics, there is an estimation of 100,000 to 150,000 new cases and about 75,000 deaths from cancer each year. In 2010, there were 126,307 new cancer cases, with 71,940 men and 54,367 women. It has been predicted that 200,000 new cases of cancer and 100,000 deaths each year could be observed in Vietnam 2010.[1] Hence, it is urgent to find effective therapies to treat cancers. There are four main types of cancer treatments: surgery, radiotherapy, chemotherapy, and targeted therapy. Among these, chemotherapy has been widely employed to cure patients at the final stage of cancer. Many active ingredients have been shown to be effective in treating cancer, such as busulfan, doxorubicin (DOX), 5-fluorouracil (5-FU), hydroxyurea, and letrozole.[2] However, these active ingredients have some disadvantages, such as poor targeting specificity, poor pharmacokinetics, and many side effects (due to high doses).[3]

Furthermore, these chemicals' instability, low solubility, and bioavailability also reduce the chemotherapy's efficiency for cancer treatment.[4] In order to tackle these disadvantages, the development of cancer drug-delivery systems has been extensively considered to precisely deliver the active ingredients to the targeted tumors using nanomaterials such as liposomes, micelles, polyelectrolyte capsules, and so on.[5−9] Nanomaterials could effectively encapsulate active ingredients and directly deliver them to cancer cells before releasing for effective consumption by cancer cells.[10,11] However, the capability of releasing active drugs to the tumors at the right time is one of the main disadvantages of nanomaterial-based delivery systems. To tackle this disadvantage, unique properties of nanomaterials, such as thermal and pH properties, could be employed to design the delivery systems, which could be released by controlling the heat or pH.[12,13] Modifying the nanomaterials' surfaces with functional groups such as proteases or phospholipases could also be utilized to precisely release the active ingredients to the tumor cells. Many nanomaterials have been effectively used to design drug-delivery systems.[14−17] One of the materials which have been intensively studied for drug delivery in cancer therapy is metal–organic frameworks (MOFs) or metal–organic complexes (MOCs).[7−9] The porous MOCs as carriers reveal several advantages over conventional nanocarriers (inorganic nanomaterials, quantum dots, polymers, and liposomes) such as high drug loadings, relative stability, and less side effects and toxicities.[18] This is because the MOC materials have high surface area, adjustable porosities and compositions, biode-

Received: August 30, 2022
Accepted: November 28, 2022
Published: December 9, 2022

ACS Publications

© 2022 The Authors. Published by American Chemical Society

https://doi.org/10.1021/acsomega.2c05614
ACS Omega 2022, 7, 46674–46681

gradability, efficient drug loading and controlled release, and surface modification possibility.[19,20]

MOC frameworks are commonly constructed from metal ions and organic ligands.[21,22] MOCs with reasonable specific surface areas, capable of tuning the pore size and functionalizing the inner surface properties, could be promising in many applications, including but not limited to environmental treatment, catalyst, drug delivery, medical, adsorption, and separation.[23−30] With large cell volume, high surface area, biocompatibility and degradability, mesoporous windows, and mesoporous cages, MOCs have been extensively studied for drug-delivery systems.[31−34] For example, an MOC [bioMOC-Zn(Cys)] with the tumor-sensitive biological property was successfully constructed from Zn^{2+} ions and a small biological molecule (L-cystine, Cys).[35] It was demonstrated that DOX@bioMOC-Zn(Cys) in nanoscale size accelerated the anticancer drug uptake via the endo/lysosomal pathway. In our previous work, we successfully incorporated ferric ions, trimesic acid, and poly(ethylene glycol) to produce a porous Fe-BTC-PEG MOC.[36] The prepared MOC had a maximum loading capacity of 364 mg/g for the 5-FU drug. The slow release of 5-FU-loaded MOCs in vivo media was observed to be up to 14 days. No death or signs of toxicity in mice administrated with Fe-BTC-PEG particles with dose in the range of 2−10 g/kg was observed for acute oral toxicity.

It has been well known that 5-FU is a chemotherapeutic compound, which has been widely utilized to treat head, neck, breast, and colorectal cancer. However, free-standing 5-FU has low selectivity, short half-life biological properties, and side effects, which might harm the marrow, gastrointestine, and bone.[37,38] Thus, several drug-delivery systems were developed to precisely release the drug to the right tumor cells that need to be treated.[39,40] Among these, nanoparticles such as MOFs or MOCs, carbon-based nanomaterials, aerogel, silica nanoparticles, and magnetic nanoparticles were revealed to be effective carriers for the delivery of the 5-FU drug.[25,41−43] MOCs with a large cell volume, high surface area, biocompatibility and degradability, mesoporous windows, and mesoporous cages have been considered promising carriers for 5-FU delivery. However, fabrication of the iron-1,4-benzenedicarboxylic-polyethylene glycol (Fe-BDC-PEG) MOC and utilization for the 5-FU delivery have not yet been studied before.

Herein, the green ultrasonicating approach is employed to prepare MOCs. The resultant Fe-BDC-PEG is thoroughly characterized and studied for the 5-FU drug delivery. The 5-FU-loaded Fe-BDC-PEG MOCis administered in mice to evaluate the acute and repeated dose 7 day oral toxicity. The effect of 5-FU-loaded Fe-BDC-PEG on several cancer cells is also investigated.

RESULTS AND DISCUSSION

Material Characterization. Figure 1 shows the X-ray diffraction (XRD) pattern of the Fe-BDC-PEG complex to study the crystalline nature of the material. It can be seen that the material sample analyzed with a sweep angle of 5−30° has a form similar to Fe-BDC-PEG reported previously.[44] The main peaks of Fe-BDC-PEG were at 5.56, 9.19, and 10.58. The XRD pattern of the sample reveals that the crystal phase of the product is Fe-BDC-PEG with a monoclinic symmetry.[45] The XRD pattern of the Fe-BDC material (Figure S1) reveals diffraction peaks similar to that of the Fe-BDC-PEG complex, indicating the successful formation of the complex.

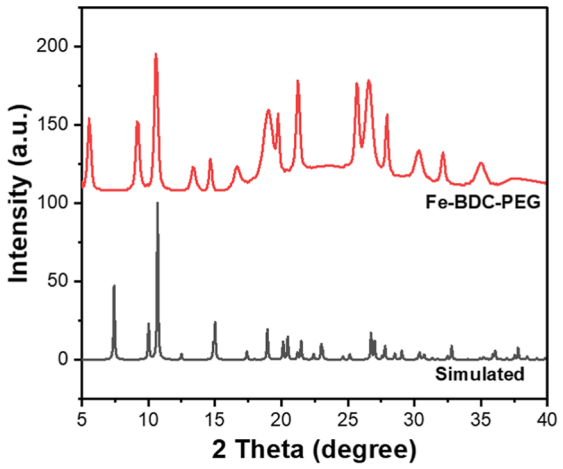

Figure 1. XRD pattern of the Fe-BDC-PEG material.

The morphology of the synthesized material was observed by scanning electron microscopy (SEM) and transmittance electron microscopy (TEM), and the result is shown in Figure 2. SEM and TEM images (Figure 2a,b) show that the Fe-BDC-PEG crystals synthesized with ultrasound conditions are uniform and relatively small in particle size. The prepared Fe-BDC-PEG complexes are in octahedron shape with diameter in the range of 20−50 nm, a length of 50−150 nm, and in the "inhaled" state. These results prove that the flexible structure of Fe-BDC-PEG, as well as particle sizes with open pores, are suitable for the reception of guest molecules for drug-delivery systems. The EDS spectrum illustrated in Figure 2c confirms the Fe, C, and O presence in the Fe-BDC-PEG complex with elemental composition appropriate with the stoichiometry ratio in the complexes.

FTIR spectroscopy investigated the bonding nature and functional groups in the Fe-BDC-PEG complex, and the result is exhibited in Figure 3. The broad characteristic band at 3415 cm^{-1} is attributed to the stretching vibration of the O−H group in absorbed water as well as in the PEG and BDC molecules. The characteristic peaks at 1686 and 524 cm^{-1}, which are typical for the stretching vibration of C═O in the H_2BDC compound, are not observed, demonstrating the absence of H_2BDC in the prepared complex. The absorption bands that appeared at 1617, 1384, and 772 cm^{-1} are assigned to the asymmetric and symmetric stretching vibrations of $-COO^-$and 1-4-substituted benzene core of BDC^{-2}.[46] The probe of Fe−O bonding is observed by the presence of an absorption peak at around 540 cm^{-1}. These vibration bands of the BDC and Fe−O were also observed in the FTIR spectrum of the Fe-BDC MOFs as shown in Figure S2. The characteristic absorption bands of PEG also appear in the FTIR spectrum of the complex, proving the successful incorporation of the PEG molecule in the complex. These results indicate that ferric ions successfully coordinate with BDC^{2-} ligands in the presence of PEG to form the Fe-BDC-PEG MOC.

Illustrated in Figure 4 is the N_2 adsorption isotherm of the Fe-BDC-PEG material, which was employed to calculate the surface area of the material. The N_2 adsorption and desorption isotherms of the Fe-BDC-PEG were obtained at a temperature of 393 K, and the specific surface area was determined using the Brunauer−Emmett−Teller (BET) method. The BET surface area of Fe-BDC-PEG is determined to be approx-

https://doi.org/10.1021/acsomega.2c05614
ACS Omega 2022, 7, 46674−46681

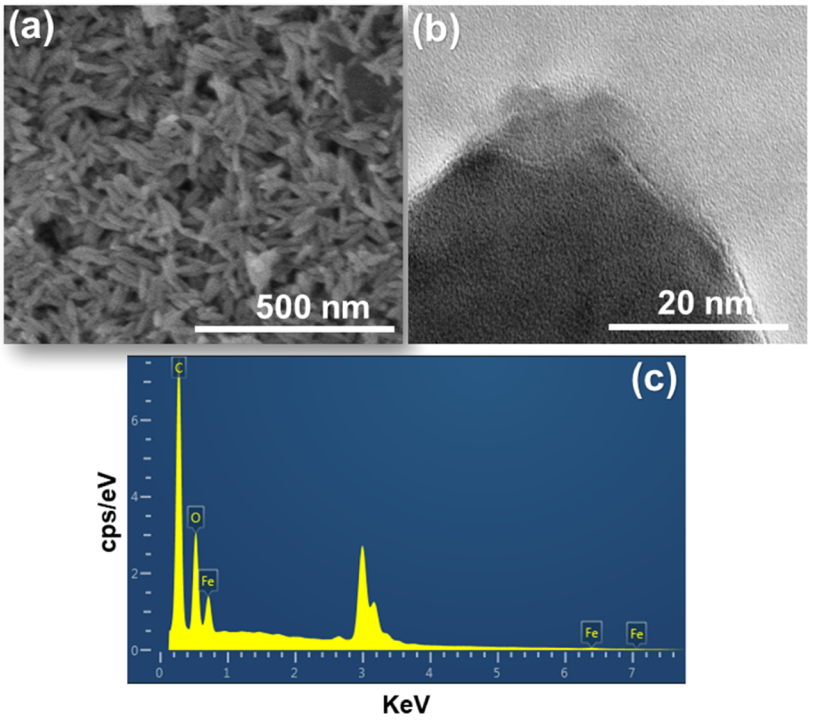

Figure 2. (a) SEM image, (b) TEM image, and (c) EDX spectrum of the Fe-BDC-PEG material.

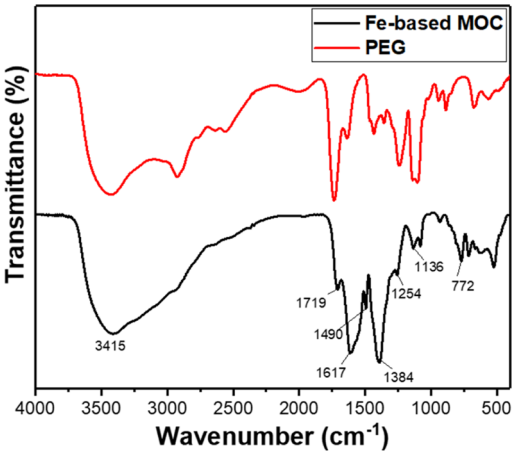

Figure 3. FTIR spectra of PEG (red line) and Fe-BDC-PEG (black line) material.

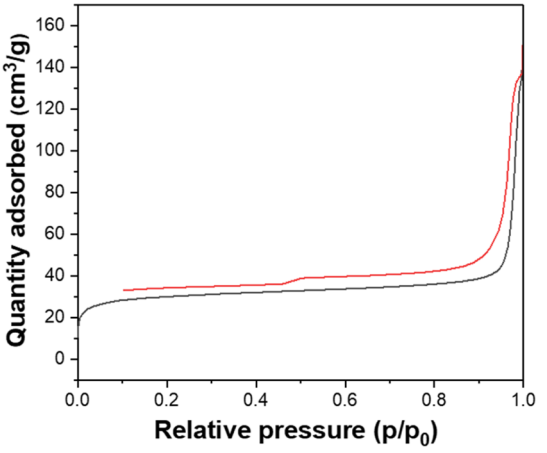

Figure 4. N_2 adsorption isotherm pattern of the Fe-BDC-PEG material.

imately 108.9 m^2/g with the pore volume and pore diameter of 0.206 cm^3/g and 7.58 nm, respectively. This pore diameter has been demonstrated to be appropriate for the loading of small drug molecules such as 5-FU. The low surface area of the material might be due to the existence of the material in the "inhaled" state; it shrinks deep into the hollow framework, which limits the N_2 adsorption ability of the material. These hypotheses have also been studied and reported previously. The drug loading-release experiments were conducted to evaluate the drug-loading ability and morphology of the after-loading, with the results presented in the next section.

Drug Loading-Release Ability Evaluation. It has been well known that 5-FU has been widely employed in the treatment of colorectal, stomach, and breast cancers. The prepared Fe-BDC-PEG complex has a particle size, surface area, pore volume, and pore diameter which are suitable for delivering the 5-FU drug to minimize the side effect of overdose as well as nontargeted treatment. More importantly, the integration of PEG in the complex enables more functional groups to bind with the drugs; as a result, more drug could be loaded in the Fe-BDC-PEG complex compared to that of Fe-BDC. For drug delivery, the loading capacity of drugs is one of the decisive factors in assessing the material's applicability. The loading capacity of the Fe-BDC-PEG complex for the 5-FU drug was determined by immersion of the complex in 5-FU solution until reaching an equilibrium adsorption state. The difference in weights of material before and after loading was used to calculate the maximal capacity of drug loading. The maximal loading of the prepared Fe-BDC-PEG for the 5-FU drug was calculated to be approximately 348.22 mg/g complex, which is higher than the loading capacity of the Fe-BDC material (251.3 mg/g). This high 5-FU loading of Fe-BDC-PEG is comparable with that of the Fe-BTC-PEG complex and reasonable for drug-delivery purpose.[36,47]

https://doi.org/10.1021/acsomega.2c05614
ACS Omega 2022, 7, 46674−46681

One of the main properties of advanced materials that is effectively used for drug delivery is slow release on purpose. For the drug-release test, the loaded material was immersed in different pH solutions of phosphate-buffered saline PBS (pH 7.4, 6.8, and 5), and 5-FU concentration was determined by UV−vis spectrometry at a wavelength of λ_{max} = 266 nm. The results of the drug release in different pH solutions are shown in Figure 5. It is obvious from the figure that the releasing

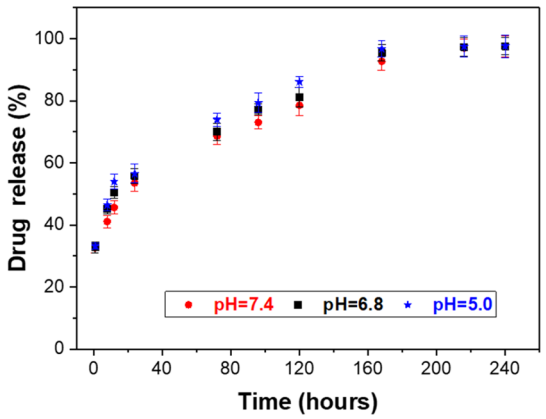

Figure 5. 5-FU concentration corresponding to the soaking time of 5-FU-loaded material in different pH solutions. The activity of the Fe-BDC-PEG@5-FU system on cancer cells.

profiles of the 5-FU drug from the loaded material from studied pH solutions are relatively similar. The result indicates that the 5-FU released from the material increased rapidly during the first day of the releasing experiment. The amount of drug released after 1 h in the simulated body medium was recorded to be around 113.44 mg/g. After 24 h, the amount of drug was approximately 186.15 mg/g. After this period, 5-FU was slowly released in this medium. After 7 days in the solution, the drug was almost entirely released from the material with a release efficiency of 92.69%, and after 10 days, 97.52% of 5-FU was released from the loaded Fe-BDC-PEG complex.

The cytotoxicity assay aims to screen and detect substances that inhibit the growth or destruction of cancer cells in in vitro conditions and determines the cellular protein content after dyeing with sulforhodamine B by measuring the optical density at 515−540 nm. The evaluated results of the cancer cell's suppression over time are presented in Figure 6, with IC_{50} being the concentration of drug at which 50% of the target is inhibited. The results show that the unloaded 5-FU was relatively stable in the experiment conditions and show negligibly different activities on various cancer cell lines, with IC_{50} of free-standing 5-FU in the range of 2.24−3.80 μg/ml. Fe-BDC-PEG@5-FU system shows strong inhibitory activity on breast, gastric, and colon cancer cell lines in humans (MCF7, AGS, and HT-29, respectively). The activities varied over time, and the ability to inhibit cancer cells of the drug-loaded material increased when increasing the exposure time. Among the cancer cell lines, the drug-loaded material's inhibitory ability is the highest in the breast cancer cell line. Specifically, at an exposure time of 120 h, the IC_{50} of Fe-BDC-PEG@5-FU is around 3.75 μg/mL, which is close to the inhibition level of pure 5-FU. At the same time, the existing time of 5-FU in cancer cells increased (slower release) when cooperated with Fe-BDC-PEG, which allows stronger inhibitory activity on cancer cells.

Acute and 7 Day Oral Toxicity Study. It is obvious from the results that even at the highest Fe-BDC-PEG@5-FU dose of 10,000 mg/kg body weight, no toxicity in mice was observed. No abnormal behavior or toxic symptoms was exhibited in all mice treated with Fe-BDC-PEG@5-FU at the tested doses over the 3 day observation (data not shown). Compared to the control group, the body weight, food intake, and water consumption of the mice administered with Fe-BDC-PEG were the same. The mice treated with Fe-BDC-PEG particle responded well to light and sound, moved, and ate normally with no death during the study.

In the high dose group of 10,000 mg/kg, clinical signs such as mild diarrhea were observed in two males and one female with thin appearance and slow mobility. The average body weights of mice in the two experimental groups were lower than the body weights of mice in the controlled samples. However, the terminal body weights and body weight gains of the tested mice were not significantly decreased throughout the 7 days of experiment period compared to that of the control group (Figure 7). Throughout the testing period, the mice in all groups showed no difference in food and water consumption and subchronic toxicity study (data not shown). Food and water consumption between the low-dose-treated group (2000, 4000 mg/kg), moderate-dose-treated group (6000 mg/kg), high-dose-treated group (8000, 10,000 mg/kg), and the control group was not significantly different after 72 h of treatment.

CONCLUSIONS

In short, the Fe-BDC-PEG material has been successfully synthesized by ultrasound from $FeCl_3$ salt and terephthalic acid in dimethyl formamide (DMF). The maximum 5-FU loading capacity of this material was 348.22 mg/g. The amount of drug released from the material was determined to be 92.69% after 7 days and reached a maximum value of 97.52% after 10 days. The ability to inhibit various cancer cell lines of the drug-loaded material was relatively high and increased when the exposure time increased with different levels on different cell lines. With a size of about 200−400 nm, this is a promising material for cancer therapy, especially for breast, gastric, and colon cancer cell lines in humans (MCF7, AGS, and HT-29, respectively). No death or signs of changes in locomotor activity was observed in mice administered with Fe-BDC-PEG at all dose groups for 7 days. Repeated dose oral administration of Fe-BDC-PEG at the tested doses did not compromise water and food consumption, which was observed in all mice between the first and seventh day of treatment. Since no death or signs of toxicity, such as changes in water and food intake and body weight, were observed, Fe-BDC-PEG can be considered as less toxic according to the class method recommended by the OECD 423 (OECD, 2001), fitting into class 5 (LD50 greater than 10,000 mg/kg).

EXPERIMENTAL SECTION

Materials. All chemicals were provided by Sigma-Aldrich including terephthalic acid (H_2BDC), $C_6H_4(COOH)_2$ ≥99%, iron(III) chloride hexahydrate ($FeCl_3{\cdot}6H_2O$) ≥99%, polyethylene glycol diacid 250 (PEG250diacid) ≥99.5%, ethanol (C_2H_5OH) 96%, pure 5-FU, PBS, trichloroacetic acid, and sulforhodamine B. Tools and equipment such as the telsonic

https://doi.org/10.1021/acsomega.2c05614
ACS Omega 2022, 7, 46674−46681

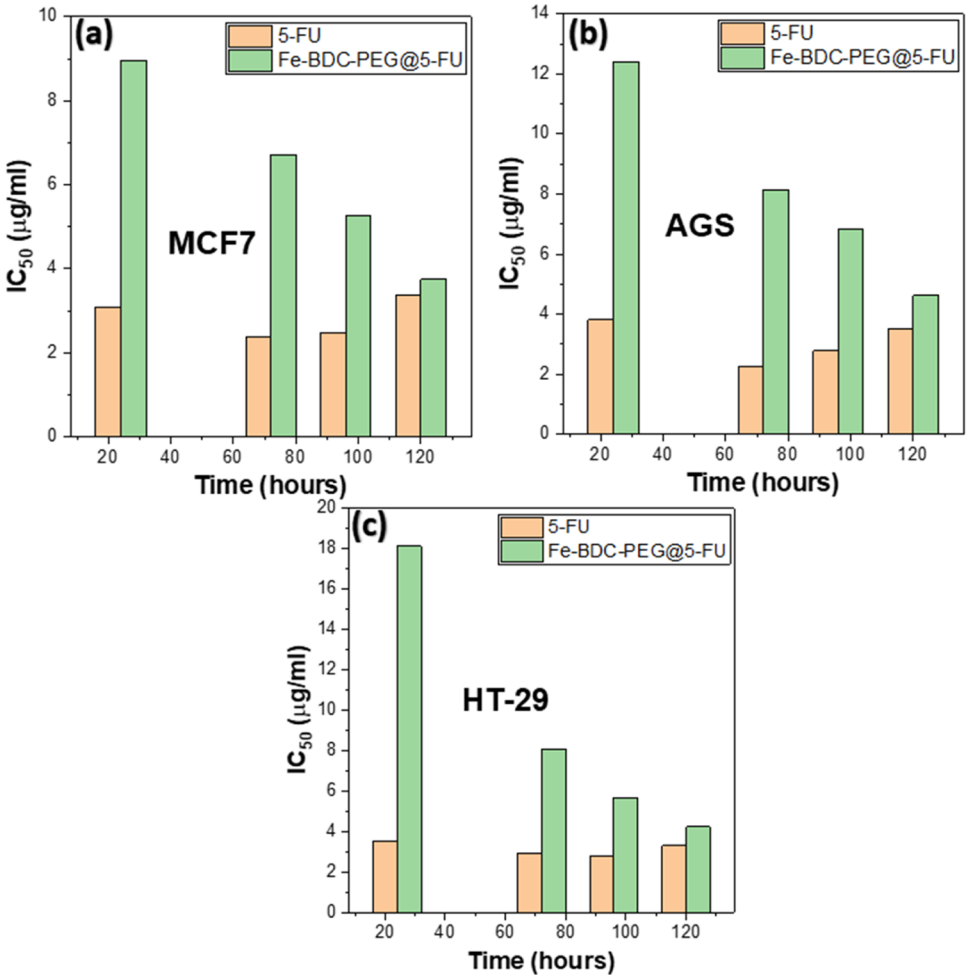

Figure 6. Cytotoxicity data for Fe-BDC-PEG@5-FU compared with pristine 5-FU in (a) breast (MCF7), (b) gastric (AGS), and (c) colon (HT-29) cancer cell lines in humans.

ultrasonic tank 50/60 Hz, the Hettich Zentrifugen centrifuge EBA21, the Ketone 101 drying oven type 300±1 °C, the Petrotest thermostat, and laboratory glass wares were employed for all experiments.

Preparation of Material. The synthesis process is adopted from previous work.[44] Typically, ferric chloride hexahydrate (1.35 g) was dissolved in 5 mL of DMF to obtain solution A. Solution B was prepared by dissolving H_2BDC (0.83 g) and 1.25 mL of PEG250 in 20 mL of DMF. Each solution was stirred separately for 15 min and then mixed and sonicated for 7 h. The white precipitate was filtered and thoroughly washed with boiling DMF and ethanol/water mixture (ratio of 1:1) and dried at 80 °C for 6−8 h.

A drug-loading experiment was carried out with 0.01 g of material in 10 mL of 5-FU 1 g/L for 72 h. The product was filtered and dried at 80 °C for 3 h.

Characterizations. The chemical composition of the material was characterized by the XRD technique on X'Pert Pro equipment at the Institute of Chemistry and Materials, Academy of Military Science and Technology. The morphology and size of the material were characterized by SEM at the Institute of Materials Science, Vietnam Academy of Science and Technology. The material's surface parameters were evaluated by nitrogen sorption experiments based on the BET equation at the Institute of Chemistry, Vietnam Academy of Science and Technology. The drug loading and release ability of the material was evaluated by UV−vis spectrophotometry at the Department of Chemistry, Hanoi University of Science with PBS solution in which the drug-loading material was soaked at λ_{max} = 266 nm. The equation of the 5-FU calibration curve is defined as $C = 50 \times (4.69 \times \text{Abs} + 1.003)$, where C is the concentration of the 5-FU solution.

The loading capacity was determined by immersing the prepared Fe-BDC-PEG material into the 5-FU-containing solution with a 5-FU concentration of 10 g/L in 72 h to determine the loading capacity of the sample for 5-FU.

To determine the drug-release ability, 0.01 g of the loaded material was soaked in 10 mL of PBS solution at 37 °C at different times, and 5-FU concentration was measured. The amount of drug released from the material in this medium is calculated by the formulation

$$Q = m_{5-FU}/m_{Fe-BDC-PEG}(g/g)$$

To calculate the release efficiency of the loaded material following the formulation

$$H_{ome} = 100 \times Q/Q_{max}\ (\%)$$

where Q_{max} is the maximum loading capacity of the material.

The cancer cell inhibition ability was evaluated by an in vitro cytotoxic assay designed by the National Cancer Institute on three human cancer cell lines: gastric carcinoma—AGS, breast carcinoma−MCF7, and colorectal adenocarcinoma—HT-29.

https://doi.org/10.1021/acsomega.2c05614
ACS Omega 2022, 7, 46674−46681

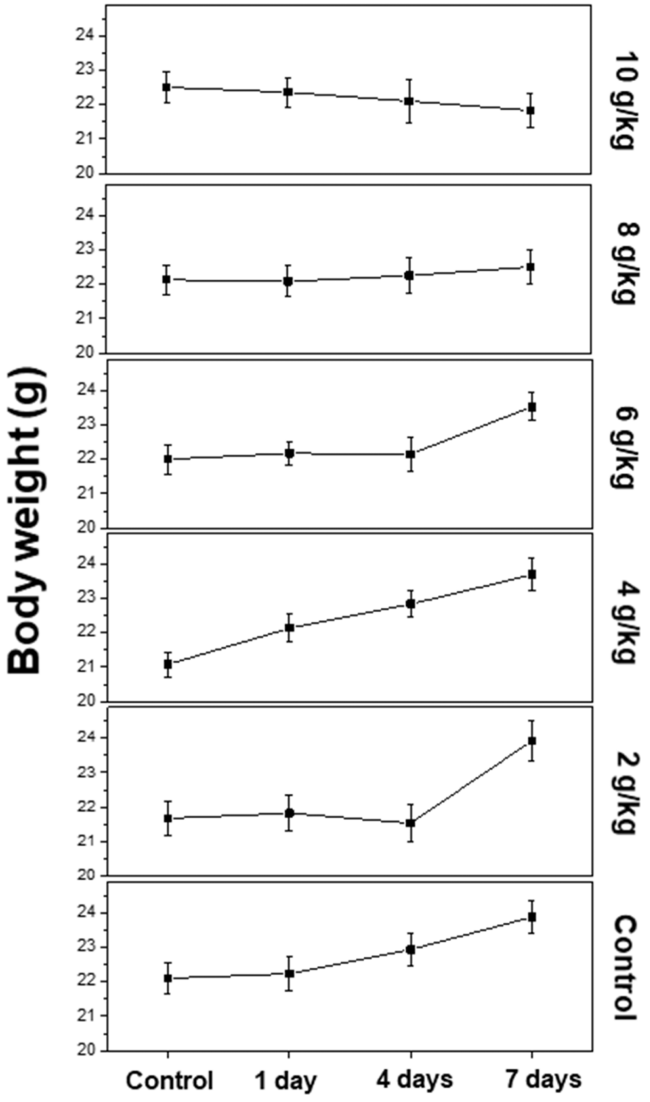

Figure 7. Body weight change in mice treated with Fe-BDC-PEG complex with various doses for 7 days.

The experiments were performed at the Institute of Biotechnology, Vietnam Academy of Science and Technology.

Acute Oral Toxicity Study. The mice (Albino BALB/c) used for the oral toxicity study were provided by the Institute of Biotechnology, Vietnam Academy of Science and Technology (Hanoi, Vietnam) with an age of 8 weeks and a weight of 19−22 g. All mice lived in a temperature-controlled room with a 12 h light and dark cycle. The ethical guidelines (Vietnamese ethical laws and European Communities Council Directives of November 24, 1986 (86/609/EEC) for the care and use of laboratory animals were employed for all experiments.

The acute oral toxicity of the Fe-BDC-PEG MOC was investigated following OECD GUIDELINE 425.[48] A stomach tube was used to introduce Fe-BTC-PEG into mice with various doses of 2000, 4000, 6000, 8000, and 10,000 mg/kg body weight after 12 h diet. The survival rate and toxic symptoms in mice were observed every 3 days.

OECD Test Guideline 407 and Taiwan Food and Drug Administration (2014)[48] were employed to determine the 28 day oral toxicity test. Seven groups of 6 mice were administered Fe-BDC-PEG with doses of 0, 2, 4, 6, 8, and 10 g material/kg body weight for 7 consecutive days. The controlled mice only took water. The daily observation was used to evaluate the general appearance of all mice. Food consumption was assessed on the first day, the fourth day, and the seventh day of the experiment, with body weights measured daily.

■ ASSOCIATED CONTENT

Supporting Information

The Supporting Information is available free of charge at https://pubs.acs.org/doi/10.1021/acsomega.2c05614.

XRD pattern of the Fe-BDC metal−organic frameworks (PDF)

■ AUTHOR INFORMATION

Corresponding Authors

Phuong Thi Hoai Nguyen − *Institute of Chemistry and Materials, Hanoi 100000, Vietnam*;
Email: hoaiphuong1978@gmail.com

Duong Duc La − *Institute of Chemistry and Materials, Hanoi 100000, Vietnam*; orcid.org/0000-0003-4241-4431;
Email: duc.duong.la@gmail.com

Authors

Bac Thanh Le − *Institute of Chemistry and Materials, Hanoi 100000, Vietnam*

Chau Que Nguyen − *Hanoi University of Pharmacy, Ha Noi 100000, Vietnam*

Phuong Thi Nguyen − *Institute of Chemistry and Materials, Hanoi 100000, Vietnam*

Ha Duc Ninh − *Institute of Chemistry and Materials, Hanoi 100000, Vietnam*

Tri Minh Le − *Institute of Chemistry and Materials, Hanoi 100000, Vietnam*

Complete contact information is available at: https://pubs.acs.org/10.1021/acsomega.2c05614

Author Contributions

The manuscript was written with the contributions of all authors. All authors have given approval for the final version of the manuscript.

Notes

The authors declare no competing financial interest.

■ ACKNOWLEDGMENTS

This study was funded by the 562 Program ("Basic Science Development in the fields of life, earth, and marine science in the period of 2017−2025 orienting to 2030"), grant no. ĐTĐL.CN-72/19.

■ REFERENCES

(1) Ministry of Health. *National Strategy for Non-communicable Disease Prevention for the Years 2015−2025*; Ministry of Health, 2015; pp 51−52.

(2) Kinh Van, N.; Tuan, A. N.*Modern Approaches-Gel for Cancer Treatment*; Medical Publishing House, 2011.

(3) Bray, F.; Ferlay, J.; Soerjomataram, I.; Siegel, R. L.; Torre, L. A.; Jemal, A. Global cancer statistics 2018: GLOBOCAN estimates of incidence and mortality worldwide for 36 cancers in 185 countries. *Ca-Cancer J. Clin.* **2018**, *68*, 394−424.

(4) Allen, T. M.; Cullis, P. R. Drug delivery systems: entering the mainstream. *Science* **2004**, *303*, 1818−1822.

(5) Giménez-Marqués, M.; Serre, C.; Horcajada, P. Nanostructured metal-organic frameworks and their bio-related applications. *Coord. Chem. Rev.* **2016**, *307*, 342−360.
(6) Horcajada, T. C.; Chalati, C.; Serre, B.; Gillet, C.; Sebrie, T.; Baati, J. F.; Eubank, D.; Heurtaux, C.; Clayette, C.; Kreuz, K.; Chang, V.; Hwang, P.-N.; Marsaud, L.; Bories, S.; Cynober, G.; Gil, P.; Férey, R.; Couvreur, P.; Gref, R. Porous metal-organic-framework nanoscale carriers as a potential platform for drug delivery and imaging. *Nat. Mater.* **2010**, *9*, 172−178.
(7) Beg, S.; Rahman, M. Nanoporous metal organic frameworks as hybrid polymer-metal composites for drug delivery and biomedical applications. *Drug Discovery Today* **2017**, *22*, 625.
(8) Chowdhury, F. Y.; Yusof, F.; Salim, W. W. A. W.; Sulaiman, N.; Faruck, M. O. An overview of drug delivery vehicles for cancer treatment: Nanocarriers and nanoparticles including photovoltaic nanoparticles. *J. Photochem. Photobiol., B* **2016**, *164*, 151−159.
(9) Díaz, M.; Vivas-Mejia, P. Nanoparticles as Drug Delivery Systems in Cancer Medicine: Emphasis on RNAi-Containing Nanoliposomes. *Pharmaceuticals* **2013**, *6*, 1361−1380.
(10) Chamundeeswari, M.; Jeslin, J.; Verma, M. L. Nanocarriers for drug delivery applications. *Environ. Chem. Lett.* **2019**, *17*, 849−865.
(11) Maeda, H.; Nakamura, H.; Fang, J. The EPR effect for macromolecular drug delivery to solid tumors: Improvement of tumor uptake, lowering of systemic toxicity, and distinct tumor imaging in vivo. *Adv. Drug Delivery Rev.* **2013**, *65*, 71−79.
(12) Sun, W.; Chen, X.; Xie, C.; Wang, Y.; Lin, L.; Zhu, K.; Shuai, X. Co-delivery of doxorubicin and Anti-BCL-2 siRNA by pH-responsive polymeric vector to overcome drug resistance in in vitro and in vivo hepg2 hepatoma model. *Biomacromolecules* **2018**, *19*, 2248−2256.
(13) Gong, X.; Zhang, Q.; Gao, Y.; Shuang, S.; Choi, M. M.; Dong, C. Phosphorus and nitrogen dual-doped hollow carbon dot as a nanocarrier for doxorubicin delivery and biological imaging. *ACS Appl. Mater. Interfaces* **2016**, *8*, 11288−11297.
(14) Yang, Y.; Wang, S.; Wang, Y.; Wang, X.; Wang, Q.; Chen, M. Advances in self-assembled chitosan nanomaterials for drug delivery. *Biotechnol. Adv.* **2014**, *32*, 1301−1316.
(15) Li, J.; Cai, C.; Li, J.; Li, J.; Li, J.; Sun, T.; Wang, L.; Wu, H.; Yu, G. Chitosan-based nanomaterials for drug delivery. *Molecules* **2018**, *23*, 2661.
(16) Hubbell, J. A.; Chilkoti, A. Nanomaterials for drug delivery. *Science* **2012**, *337*, 303−305.
(17) Karimi, M.; Mansouri, M. R.; Rabiee, N.; Hamblin, M. R.*Advances in Nanomaterials for Drug Delivery*; Morgan & Claypool Publishers, 2018.
(18) He, S.; Wu, L.; Li, X.; Sun, H.; Xiong, T.; Liu, J.; Huang, C.; Xu, H.; Sun, H.; Chen, W.; Gref, R.; Zhang, J. Metal-organic frameworks for advanced drug delivery. *Acta Pharm. Sin. B* **2021**, *11*, 2362−2395.
(19) Chu, C.; Su, M.; Zhu, J.; Li, D.; Cheng, H.; Chen, X.; Liu, G. Metal-organic framework nanoparticle-based biomineralization: a new strategy toward cancer treatment. *Theranostics* **2019**, *9*, 3134.
(20) Wang, X.; Chen, X. Z.; Alcântara, C. C.; Sevim, S.; Hoop, M.; Terzopoulou, A.; de Marco, C.; Hu, C.; de Mello, A. J.; Furukawa, P.; Nelson, B. J.; Puigmartí-Luis, J.; Pané, S. MOFBOTS: metal−organic-framework-based biomedical microrobots. *Adv. Mater.* **2019**, *31*, 1901592.
(21) Yılmaz, E.; Sert, E.; Atalay, F. S. Synthesis, characterization of a metal organic framework: MIL-53 (Fe) and adsorption mechanisms of methyl red onto MIL-53 (Fe). *J. Taiwan Inst. Chem. Eng.* **2016**, *65*, 323−330.
(22) Yang, Q. X.; Xu, H.-L.; Jiang, H.-L. Metal−organic frameworks meet metal nanoparticles: synergistic effect for enhanced catalysis. *Chem. Soc. Rev.* **2017**, *46*, 4774−4808.
(23) Beg, M. R.; Rahman, M.; Jain, A.; Saini, S.; Midoux, P.; Pichon, C.; Ahmad, F. J.; Akhter, S. Nanoporous metal organic frameworks as hybrid polymer-metal composites for drug delivery and biomedical applications. *Drug Discov. Today* **2017**, *22*, 625−637.
(24) Horcajada, T. C.; Chalati, C.; Serre, B.; Gillet, C.; Sebrie, T.; Baati, J. F.; Eubank, D.; Heurtaux, C.; Clayette, C.; Kreuz, K.; Chang, V.; Hwang, P.-N.; Marsaud, L.; Bories, S.; Cynober, G.; Gil, P.; Férey, R.; Couvreur, P.; Gref, R. Porous metal-organic-framework nanoscale carriers as a potential platform for drug delivery and imaging. *Nat. Mater.* **2010**, *9*, 172−178.
(25) Keskin, S. K.; Kızılel, S. Biomedical Applications of Metal Organic Frameworks. *Ind. Eng. Chem. Res.* **2011**, *50*, 1799−1812.
(26) Kim, S.-T. Y.; Yang, S.-T.; Choi, S. B.; Sim, J.; Kim, J.; Ahn, W.-S. Control of catenation in CuTATB-n metal-organic frameworks by sonochemical synthesis and its effect on CO2 adsorption. *J. Mater. Chem.* **2011**, *21*, 3070−3076.
(27) Li, R. J. K.; Kuppler, H.-C.; Zhou, H.-C. Selective gas adsorption and separation in metal−organic frameworks. *Chem. Soc. Rev.* **2009**, *38*, 1477−1504.
(28) Li, J.-R.; McCarthy, M.; Sculley, J.; Yu, J.; Jeong, H.-K.; Balbuena, P. B.; Zhou, H.-C. Carbon dioxide capture-related gas adsorption and separation in metal-organic frameworks. *Coord. Chem. Rev.* **2011**, *255*, 1791−1823.
(29) Corma, A.; Xamena, F. X. Engineering Metal Organic Frameworks for Heterogeneous Catalysis. *Chem. Rev.* **2010**, *110*, 4606−4655.
(30) Zhu, X.-Q. L.; Liu, H.-L.; Jiang, L.-B.; Sun, L.-B. Metal-Organic Frameworks for Heterogeneous Basic Catalysis. *Chem. Rev.* **2017**, *117*, 8129−8176.
(31) Hong, Y. K. H.; Hwang, C.; Serre, G.; Chang, J.-S. Porous Chromium Terephthalate MIL-101 with Coordinatively Unsaturated Sites: Surface Functionalization, Encapsulation, Sorption and Catalysis. *Adv. Funct. Mater.* **2009**, *19*, 1537−1552.
(32) Chowdhuri, A. R.; Singh, T.; Ghosh, S. K.; Sahu, S. K. Carbon dots embedded magnetic nanoparticles@ chitosan@ metal organic framework as a nanoprobe for pH sensitive targeted anticancer drug delivery. *ACS Appl. Mater. Interfaces* **2016**, *8*, 16573−16583.
(33) Tan, L. L.; Li, H.; Zhou, Y.; Zhang, Y.; Feng, X.; Wang, B.; Yang, Y. W. Zn2+-triggered drug release from biocompatible zirconium MOFs equipped with supramolecular gates. *Small* **2015**, *11*, 3807−3813.
(34) Wu, Y. n.; Zhou, M.; Li, S.; Li, Z.; Li, J.; Wu, B.; Li, G.; Li, F.; Guan, X. Magnetic metal−organic frameworks: γ-Fe2O3@ MOFs via confined in situ pyrolysis method for drug delivery. *Small* **2014**, *10*, 2927−2936.
(35) Jiang, Z.; Wang, T.; Yuan, S.; Wang, M.; Qi, W.; Su, R.; He, Z. A tumor-sensitive biological metal−organic complex for drug delivery and cancer therapy. *J. Mater. Chem. B* **2020**, *8*, 7189−7196.
(36) Nguyen, P. T. H.; Le, B. T.; Ninh, H. D.; La, D. D. Ultrasonic-Assisted Synthesis of Fe−BTC−PEG Metal−Organic Complex: An Effective and Safety Nanocarrier for Anticancer Drug Delivery. *ACS Omega* **2021**, *6*, 33419−33427.
(37) Arias, J. L. Novel strategies to improve the anticancer action of 5-fluorouracil by using drug delivery systems. *Molecules* **2008**, *13*, 2340−2369.
(38) Jain, K. K.Drug delivery systems-an overview. *Drug Delivery Systems*; Humana Press, 2008; pp 1−50.
(39) Luo, H.; Li, C.; Zhu, Y.; Xiong, G.; Wan, Y. Layered nanohydroxyapatite as a novel nanocarrier for controlled delivery of 5-fluorouracil. *Int. J. Pharm.* **2016**, *513*, 17−25.
(40) Pan, T.-T. J.; Jia, Q.-X.; Huang, Y.-Y.; Qiu, J.; Xu, P.-H.; Yin, T.; Liu, T. Mesoporous silica nanoparticles (MSNs)-based organic/inorganic hybrid nanocarriers loading 5-Fluorouracil for the treatment of colon cancer with improved anticancer efficacy. *Colloids Surf., B* **2017**, *159*, 375−385.
(41) Ehi-Eromosele, B. I.; Ita, B. I.; Iweala, E. E. J. Silica coated LSMO magnetic nanoparticles for the pH-Responsive delivery of 5-Fluorouracil anticancer drug. *Colloids Surf., A* **2017**, *530*, 164−171.
(42) Zhu, T. Y.; Ye, J.; Liu, P.; Peng, S.; Xu, J.; Lei, H.; Deng, B.; Li, B. Nanogels fabricated by lysozyme and sodium carboxymethyl cellulose for 5-fluorouracil controlled release. *Int. J. Pharm.* **2013**, *441*, 721−728.
(43) Thi, H. P. N.; Ngoc, T. T. Investigation in loading 5-fluorouracil ability of iron-organic frameworks. *Vietnam J. Sci. Technol.* **2018**, *56*, 219−227.

https://doi.org/10.1021/acsomega.2c05614
ACS Omega 2022, 7, 46674−46681

(44) Gordon, H. K.; Kazemian, H.; Rohani, S. Rapid and efficient crystallization of MIL-53(Fe) by ultrasound and microwave irradiation. *Microporous Mesoporous Mater.* **2012**, *162*, 36−43.
(45) Yılmaz, E.; Sert, E. Synthesis, characterization of a metal organic framework: MIL-53 (Fe) and adsorption mechanisms of methyl red onto MIL-53 (Fe). *J. Taiwan Inst. Chem. Eng.* **2016**, *65*, 323−330.
(46) Lou, X.; Hu, H.; Li, C.; Hu, X.; Li, T.; Shen, M.; Chen, Q.; Hu, B. Capacity control of ferric coordination polymers by zinc nitrate for lithium-ion batteries. *RSC Adv.* **2016**, *6*, 86126−86130.
(47) Gao, X.; Hai, X.; Baigude, H.; Guan, W.; Liu, Z. Fabrication of functional hollow microspheres constructed from MOF shells: Promising drug delivery systems with high loading capacity and targeted transport. *Sci. Rep.* **2016**, *6*, 37705.
(48) Acute Oral Toxicity—Up-and-Down Procedure*OECD Guideline for Testing of Chemicals*, 2001.

https://doi.org/10.1021/acsomega.2c05614
ACS Omega 2022, 7, 46674−46681